OCEANOGRAPHY

Reframing the carbon cycle of the subpolar Southern Ocean

Graeme A. MacGilchrist[1]*†, Alberto C. Naveira Garabato[2], Peter J. Brown[3], Loïc Jullion[4], Sheldon Bacon[3], Dorothee C. E. Bakker[5], Mario Hoppema[6], Michael P. Meredith[7], Sinhué Torres-Valdés[6]

Global climate is critically sensitive to physical and biogeochemical dynamics in the subpolar Southern Ocean, since it is here that deep, carbon-rich layers of the world ocean outcrop and exchange carbon with the atmosphere. Here, we present evidence that the conventional framework for the subpolar Southern Ocean carbon cycle, which attributes a dominant role to the vertical overturning circulation and shelf-sea processes, fundamentally misrepresents the drivers of regional carbon uptake. Observations in the Weddell Gyre—a key representative region of the subpolar Southern Ocean—show that the rate of carbon uptake is set by an interplay between the Gyre's horizontal circulation and the remineralization at mid-depths of organic carbon sourced from biological production in the central gyre. These results demonstrate that reframing the carbon cycle of the subpolar Southern Ocean is an essential step to better define its role in past and future climate change.

INTRODUCTION

The subpolar Southern Ocean, south of the Antarctic Circumpolar Current (ACC), is arguably the most important region on Earth for the cycling of carbon on centennial to millennial time scales (*1*). Atmospheric carbon dioxide (CO_2) exhibits strong sensitivity to the physical and biogeochemical dynamics of the region in paleoclimatic observations (*2*), low-complexity box models (*3*, *4*), and fully three-dimensional numerical simulations (*5*, *6*). Furthermore, in the present day, the regional uptake of anthropogenic carbon is a major contributor to its storage in the deep ocean (*7*, *8*). Consequently, understanding the dynamics and variability of the subpolar Southern Ocean carbon cycle, and the system's susceptibility to change, is a fundamental challenge facing modern climate research.

The significance of the subpolar Southern Ocean in the global carbon cycle stems from its unique connection to the lower cell of the global overturning circulation (*1*). The vast carbon content of this lower cell, which occupies the deep and abyssal layers in most of the world ocean, is gradually built up by the remineralization of sinking organic matter (*9*), with some moderation by the slow upward mixing of carbon across the cell's upper density interface associated with small-scale turbulence (*6*). In the subpolar Southern Ocean, the dense waters of the lower cell are exposed directly to the ocean's surface layers, allowing their carbon to be rapidly exchanged with the atmosphere. The dynamics of the carbon cycle in the region thus determine the degree to which the large carbon pool of the lower cell is able to escape to the atmosphere—in effect, whether the lid of the lower cell is open (net outgassing) or closed (net uptake) (*1*).

Understanding of the subpolar Southern Ocean carbon cycle has traditionally been considered in terms of a two-dimensional latitude-depth framework, shown schematically in Fig. 1. This framework reflects the most conspicuous features of the regional circulation, which is characterized by intense water mass transformations and vertical overturning. Water transported across the ACC in mid-depth layers, known as Circumpolar Deep Water (CDW), is rich in dissolved inorganic carbon and is both upwelled to the surface through wind-driven divergence (*10*, *11*) and conveyed to the abyss through entrainment by dense waters cascading off the continental shelf, forming Antarctic Bottom Water (AABW) (*11*, *12*). Carbon stored within the inflowing CDW may thus be partly outgassed to the atmosphere or transferred to the deep ocean, making these water mass transformations potentially critical to the partitioning of carbon between the atmospheric and oceanic reservoirs. This overturning-centric perspective and, in particular, the transformation of CDW into AABW have traditionally underpinned investigations of the role of the Southern Ocean carbon cycle in global climate (*3*, *6*, *13*), while observational campaigns have largely focused on the areas of the most intense water mass transformations, biological activity, and sea-ice dynamics: the continental shelves around Antarctica (*14*–*16*).

Increasingly, key features of the subpolar Southern Ocean carbon cycle are being found to be inconsistent with this two-dimensional framework. Extensive observations of elevated concentrations of carbon in inflowing CDW relative to concentrations in outflowing surface waters and AABW (*15*, *17*) imply that, in a two-dimensional frame, the region should be a net source of carbon to the atmosphere. This is at odds with a number of recent studies, based both on budget analyses and on in situ measurements of the carbonate system, which find the subpolar Southern Ocean to be an oceanic carbon sink (*10*, *14*, *16*–*19*). A possible explanation for this fundamental discrepancy is the role played by biogeochemical processes in the open ocean—that is to say, away from the shelf seas—and the regional horizontal circulation (*20*), which in the subpolar Southern Ocean is primarily characterized by large cyclonic gyres. In the present study, we test this proposition by considering the cycling of carbon in the Weddell Gyre, an important and representative region of the subpolar Southern Ocean with respect to water mass transformation (*12*) and carbon drawdown (*7*, *10*).

RESULTS

Circulation and carbon uptake in the Weddell Gyre

Using sections of hydrographic stations that enclose the Weddell Gyre (Fig. 2A), the circulation in the region was quantified using inverse

[1]Department of Earth Sciences, University of Oxford, Oxford OX1 3AN, UK. [2]Ocean and Earth Science, University of Southampton, National Oceanography Centre, Southampton SO14 3ZH, UK. [3]National Oceanography Centre, Southampton SO14 3ZH, UK. [4]Aix-Marseille Univ, Université de Toulon, CNRS, IRD, MIO, UM 110, Marseille, France. [5]Centre for Ocean and Atmospheric Sciences, School of Environmental Sciences, University of East Anglia, Norwich NR4 7TJ, UK. [6]Alfred Wegener Institute Helmholtz Centre for Polar and Marine Research, Bremerhaven, Germany. [7]British Antarctic Survey, Cambridge CB3 0ET, UK.
*Present address: Atmospheric and Oceanic Science, Princeton University, Princeton, NJ, USA.
†Corresponding author. Email: graemem@princeton.edu

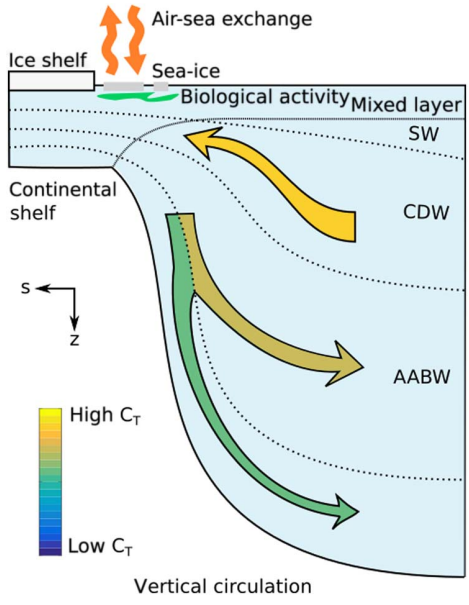

Fig. 1. Two-dimensional framework for the subpolar Southern Ocean carbon cycle. Schematic illustration of the conventional, two-dimensional, overturning-centric framework for the subpolar Southern Ocean carbon cycle. Dotted lines delineate surface water (SW), CDW, and upper and lower layers of AABW.

techniques (*11*). The horizontal circulation (Fig. 2B; presented as a cumulative sum moving clockwise around the section, with negative values indicating export of water from the region) is dominated by the cyclonic Gyre, characterized by a volume transport of 40 to 50 Sv (1 Sv = 10^6 m^3 s^{-1}). There is also a substantial horizontal throughflow of 13 ± 4 Sv, with water entering the region primarily across the eastern boundary, in the Antarctic Slope Front (ASF; Fig. 2B, station pairs 110 to 123), and leaving across the northern section (station pairs 50 to 75). The vertical circulation in the Gyre (Fig. 2C) exhibits the expected dual-overturning cell structure, with water imported in mid-depth layers (CDW and upper layers of AABW) and exported within both the surface waters and lower layers of AABW. Combining the inversion-derived velocity field with coincident measurements of total dissolved inorganic carbon (C_T; Fig. 2E) yields a residual transport of −53 ± 10 Tg C $year^{-1}$ directed out of the Gyre (*17*) that is representative of a multi-annual, summertime mean state (see Materials and Methods). The residual transport reflects the regional air-sea carbon flux, indicating that the Weddell Gyre is an important summertime sink of carbon from the atmosphere, with an estimated air-sea CO_2 uptake rate of 58 ± 10 Tg C $year^{-1}$ after accounting for dissolved inorganic carbon accumulation [through the uptake of anthropogenic carbon (*17*)] within the box. This uptake rate is consistent with that diagnosed from two other approaches (*17*), as well as with estimates from previous studies (*10*, *19*, *21*). These studies show that summertime uptake overcomes wintertime outgassing to sustain the Weddell Gyre as a substantial sink of CO_2 from the atmosphere over an annual cycle (*10*, *17*).

Comparing overturning and horizontal carbon transports

To assess the applicability of the conventional two-dimensional carbon cycle framework, we evaluate separately the contributions to regional carbon uptake made by the overturning and horizontal components of the circulation in the Weddell Gyre. This is achieved by decomposing the mass transport and carbon concentrations at the Gyre's boundary as (*22*)

$$v\rho = \overline{v\rho}^i + (v\rho)'; \quad C_T = \overline{C_T}^i + C_T' \tag{1}$$

where v is the velocity, ρ is the in situ density, overbars denote area-weighted means within neutral density layers (numbered as i), and primes denote deviations from these means. It follows that the total carbon transport across the edge of the Gyre is

$$T_C \equiv \sum_{i=1}^{n} [v\rho C_T]^i = \underbrace{\sum_{i=1}^{n} [v\rho]^i \overline{C_T}^i}_{T_C^o} + \underbrace{\sum_{i=1}^{n} [(v\rho)' C_T']^i}_{T_C^h} \tag{2}$$

where square brackets denote integration within layer i and n is the total number of discrete layers. The first term on the right-hand side is the product of the mass transport and mean carbon concentration in each layer, and quantifies the contribution of the overturning circulation to carbon drawdown in the Gyre (T_C^o). The second term arises from correlations between carbon concentration anomalies and mass transport anomalies within each layer, and thus quantifies the contribution of the horizontal circulation to regional carbon uptake (T_C^h). We use the term "horizontal" as shorthand for "within layer," which does not need to be strictly horizontal due to undulations in the layer interfaces. The horizontal component is evaluated as the residual of the total transport of carbon across the Gyre's boundary and the overturning contribution in each layer. Note that, as mesoscale eddy-induced mass transports feature explicitly in the inverse estimate of the velocity field (*11*), their contribution to carbon drawdown is included in T_C^o (see Materials and Methods).

Total carbon transport (T_C) and the transport due to the overturning circulation (T_C^o) are both associated with large mass transports in each layer such that differences between them are vanishingly small (Fig. 3A, upper panel). However, in the mass-conserved, full-depth integral—the relevant quantity for the regional air-sea carbon exchange—those differences become apparent (Fig. 3A, lower panel). The overturning circulation imports 18 ± 10 Tg C $year^{-1}$ to the Gyre, and is thus a source of CO_2 to the atmosphere, as a qualitative assessment of the vertical profiles of mass transport and carbon concentration would suggest (Fig. 2, C and D). This import of carbon to the Gyre by the overturning circulation requires that the total carbon export of −53 ± 10 Tg C $year^{-1}$ be effected by the horizontal circulation, which transports −72 ± 4 Tg C $year^{-1}$ out of the Gyre (Fig. 3B, lower panel).

In the vertical profile of T_C^h (Fig. 3B, upper panel), it is clear that a large fraction of the export by the horizontal circulation is achieved predominantly within CDW, with smaller contributions in the surface waters and upper layers of AABW. A qualitative examination of the carbon distribution in CDW (Fig. 2E) suggests that export by the horizontal circulation arises from the difference in carbon concentration between CDW imported across the Gyre's eastern boundary in the ASF (station pairs 110 to 123) and CDW exported across the Gyre's northern boundary (station pairs 50 to 75). Evaluating carbon anomaly (C_T') transports confirms that these regions account for a substantial fraction of the export of carbon by the horizontal circulation (fig. S1). Thus, the export of carbon is primarily due to the enrichment of CDW between its entry to and outflow from the Gyre.

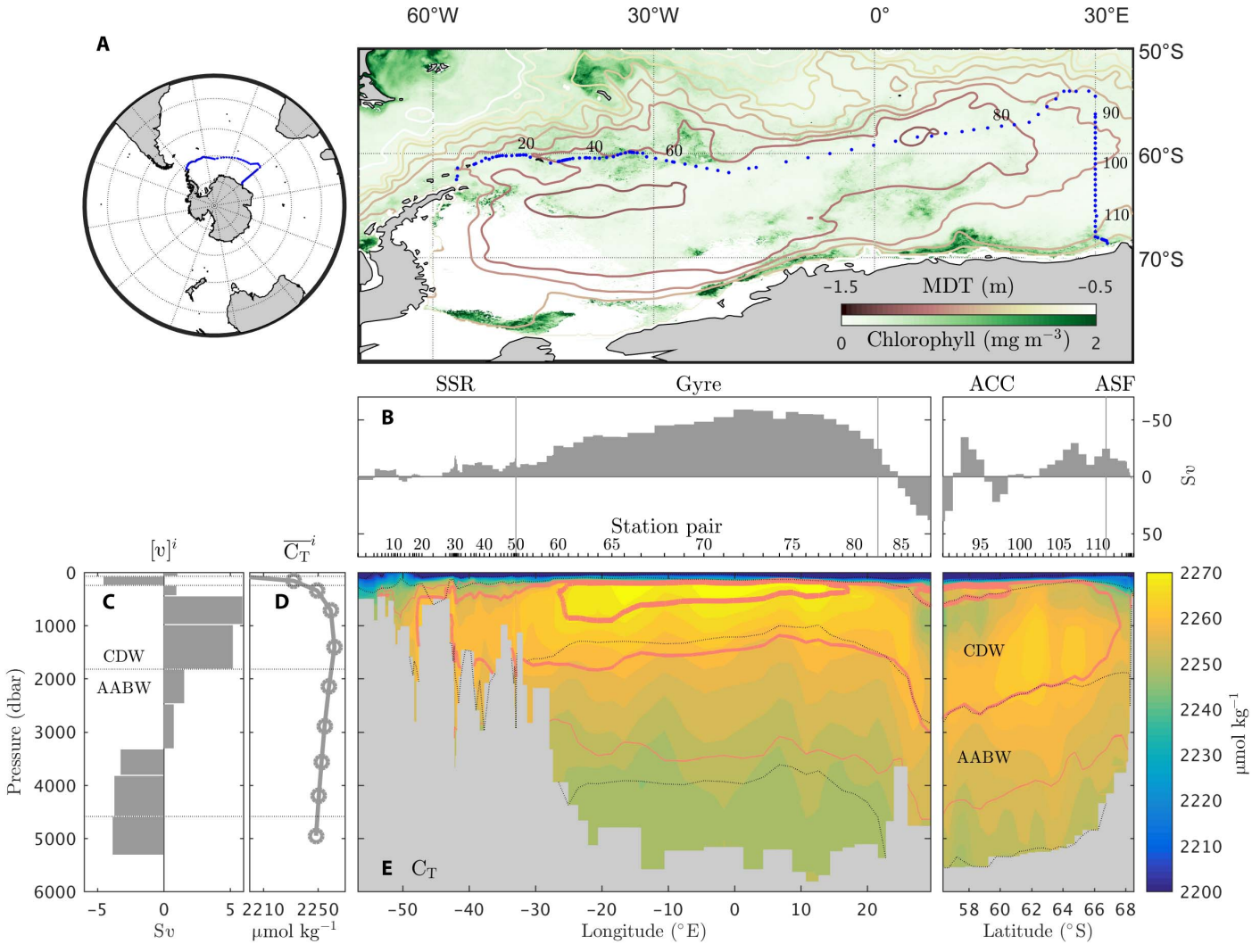

Fig. 2. Circulation and carbon in the Weddell Gyre. (**A**) Location of the Weddell Gyre and hydrographic sections. On the right panel, contours of mean dynamic topography (MDT) are plotted, revealing the cyclonic gyre circulation (contours every 0.1 m). These data are the June-July-August mean in 2005, taken from the Southern Ocean State Estimate (*41*). The 2008 annual mean chlorophyll-a concentration, derived from satellite measurements of ocean color, is also plotted (green shading) (*47*). (**B**) Cumulative horizontal circulation around the boundary of the Weddell Gyre, derived from the inversion (*11*). Volume transports for each station pair are integrated from left to right. Note the reversed direction of the *y* axis such that export is upward. (**C**) Overturning circulation in the Weddell Gyre, derived from the inversion, in neutral density layers. Bars correspond to the volume transport in each layer ($[v]^i$). The center location and thickness of each bar correspond to the mean depth and thickness of that layer. Horizontal dotted lines denote the interfaces between major water masses. (**D**) Area-weighted mean carbon concentration in each layer ($\overline{C_T}^i$). (**E**) Carbon concentration, C_T, around the Weddell Gyre. As for (C) and (D), dotted lines denote the interfaces between the major water masses. Pink contours correspond to the concentrations (80, 90, and 100 µmol kg^{-1}) of the remineralized organic matter component (C_{soft}) of the carbon partitioning formulation (see Materials and Methods), with thicker contours denoting greater concentration.

As CDW leaves the Weddell Gyre, it descends underneath the ACC as a constituent of the northward-flowing limb of the lower cell of global overturning (*12*, *23*) such that the enrichment of CDW in the Gyre acts to draw down carbon into the world ocean abyss (*20*). The significance of this mechanism in transporting carbon to the deep ocean can be determined by comparing its magnitude of ~50 Tg C year^{-1} (summing horizontal carbon transports in CDW) to the primary source of carbon into the ocean abyss—sinking particulate matter—assessed as 430 Tg C year^{-1} across the 2000-m depth horizon for the global ocean (*9*). Thus, even accounting for its operation in the Weddell Gyre alone, this mechanism is of global significance for deep-ocean carbon sequestration.

Assessing the drivers of horizontal carbon transport

The drivers of the carbon enrichment experienced by CDW as it circulates horizontally through the Weddell Gyre can be assessed with the use of a carbon partitioning approach, in which the properties of the carbon field along the Gyre's edge are attributed to a range of physical and biogeochemical processes (see Materials and Methods) (*24*, *25*). The carbon concentration contributed by the remineralization of organic matter (C_{soft}) is overlain on the distribution of C_T in Fig. 2E (pink contours at 80, 90, and 100 µmol kg^{-1}, with progressively increasing thickness). Within CDW, the coincident patterns of C_T and C_{soft} indicate that the enrichment of carbon observed across the center of the

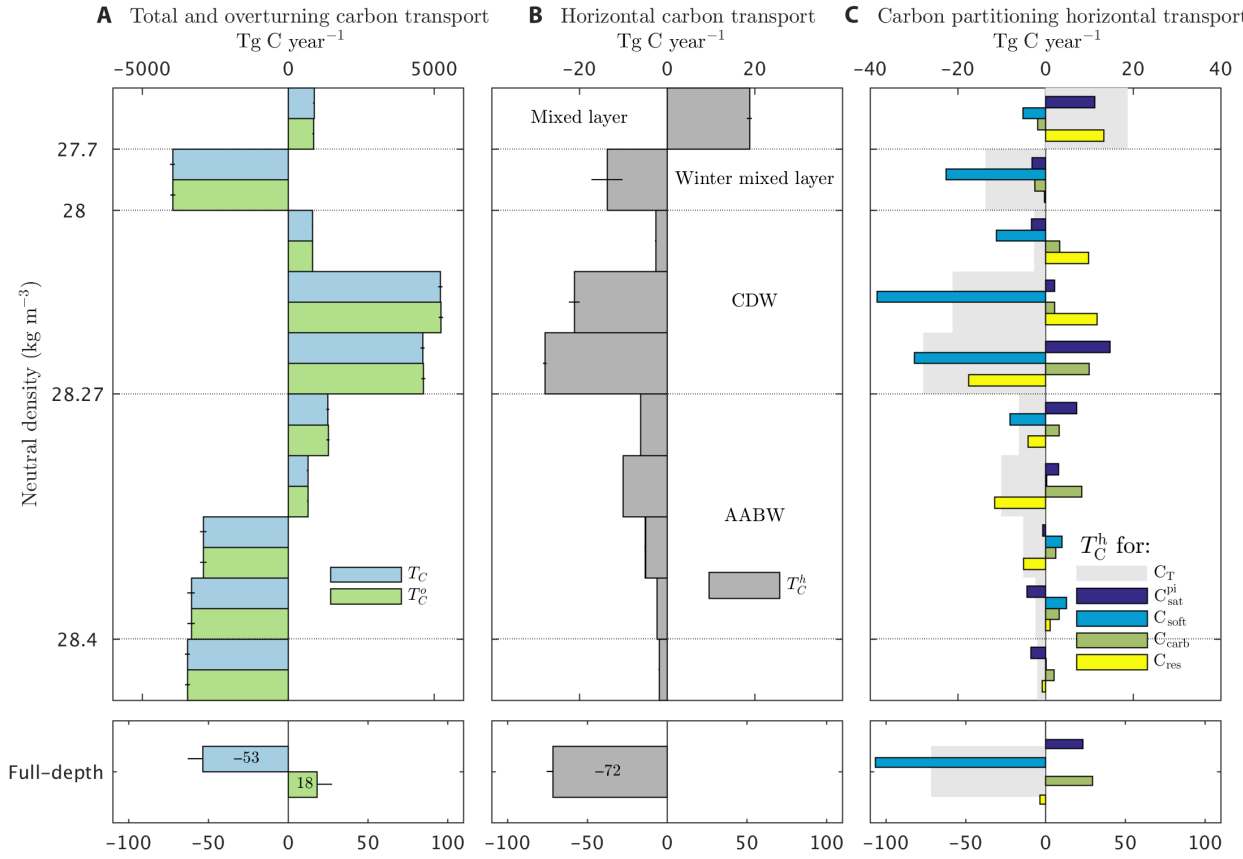

Fig. 3. Total, overturning, and horizontal carbon transports in the Weddell Gyre. (**A**) Total transport of carbon in the Gyre (T_C; blue) and the transport due to the overturning component of the circulation (T_C^o; green), for each layer (upper panel) and summed over the full depth (lower panel). Full-depth transports include export of carbon in sea ice, assuming a sea-ice carbon concentration of 600 μmol kg^{-1} (*17*). (**B**) Transport of carbon due to the horizontal component of the circulation (T_C^h), for each layer (upper panel) and summed over the full depth (lower panel). (**C**) Horizontal transport of carbon [gray bars; same as in (B)] separated into contributions from each constituent of the carbon partitioning (see Materials and Methods), for each layer (upper panel) and summed over the full depth (lower panel). Note that for all panels, the *x* axis has a different scale between the layer-wise (upper panel) and the full-depth (lower panel) transports. All of the full-depth transports (bottom panels) have the same scale.

northern section relative to carbon levels in the ASF at the Gyre's eastern boundary is caused by the remineralization of organic matter. By contrast, the other constituents of the carbon partitioning formulation (fig. S2) do not follow this pattern. This pool of biologically enriched carbon concentration in CDW has been consistently observed in the Gyre's center (*26*), where sinking organic matter from biological production in the central gyre region has been documented to remineralize at relatively shallow depths (*27*), leading to an accumulation of carbon in CDW within the Gyre's inner reaches. The relevance of this mechanism to explain our observations is reaffirmed by the correspondence of the maximum in C_{soft} along the northern section (Fig. 2E) with a minimum in chlorofluorocarbon-11 (fig. S3), a tracer of recent atmospheric contact. This supports the conclusion that the elevated levels of C_T at the Gyre's northern boundary arise from biological processes operating in the central region of the Gyre, as opposed to being a signature that was transported from the well-ventilated shelf-sea waters along the Gyre's rim.

We quantify the contribution of the biological pump to carbon uptake in the Weddell Gyre by examining the transport of each carbon constituent across the region's boundaries. The horizontal components of these transports (having again applied the decomposition of Eq. 2) are shown in Fig. 3C. As expected from the preceding discussion, the export of carbon from the Gyre via the horizontal circulation of CDW is found to be overwhelmingly associated with the transport of C_{soft} out of the region. This contribution to the regional biological carbon pump (~80 Tg C year^{-1}, summing T_C^h for C_{soft} in the three layers of CDW) compares favorably with independent estimates derived from upper-ocean nutrient budgets (~110 Tg C year^{-1}) (*17*).

The prevalence of open-ocean biological processes in the drawdown of carbon in the Weddell Gyre is somewhat unexpected in light of the more modest chlorophyll-a concentrations observed in the Gyre interior relative to that near the Antarctic continental shelves (Fig. 2A)—likely the result of greater iron limitation in the central region (*18*). However, satellite-derived estimates of net primary production integrated across the Weddell Gyre (120 to 190 Tg C year^{-1}; see Materials and Methods) indicate that as much as 80% occurs in the vast central gyre region. Sinking and remineralization of this organic matter can, therefore, completely account for the export of C_{soft} in CDW, assuming sinking efficiencies within the measured range (*27*). Together, these results suggest that open-ocean primary production is more effective at carbon drawdown than shelf-sea biological processes, making it the primary driver of regional carbon sequestration.

Cyclonic gyres such as the Weddell Gyre are a dominant feature of the horizontal circulation in the subpolar Southern Ocean. As noted

above, horizontal carbon export from the Weddell Gyre arises from the accumulation of carbon within the recirculating waters of the central gyre. Hence, it is highly plausible that the same mechanism operates in the other cyclonic gyre systems of the subpolar Southern Ocean, such as that spanning the Ross Sea. This expectation is endorsed by biogeochemical measurements along a section crossing the Ross Gyre, for which application of our carbon partitioning approach reveals the occurrence of a pool of elevated C_{soft} within CDW with concentrations comparable to and exceeding those in the Weddell Gyre (fig. S4). While a circumpolar quantification of horizontal carbon transports is not possible at present, it is reasonable to expect that the mechanism of carbon uptake here identified in the Weddell Gyre will be relevant across the other cyclonic gyres that make up the subpolar Southern Ocean.

DISCUSSION

Our observational analysis demonstrates that carbon export from the Weddell Gyre, a representative region of the subpolar Southern Ocean, is established by the accumulation within CDW of remineralized organic carbon sourced from open-ocean primary production. The central implication is that the present-day rate of carbon uptake in the subpolar Southern Ocean is set by the open-ocean biological pump and the horizontal gyre circulation. This represents a deviation from the conventional, two-dimensional perspective of the carbon cycle in the subpolar Southern Ocean (Fig. 1), which attributes a disproportionate, rate-controlling role to the overturning circulation and biological processes on the Antarctic continental shelves. Our results support a reframing of the conceptual framework of the subpolar Southern Ocean carbon cycle to bring to the fore the critical mechanisms associated with the horizontal circulation and biological processes in the central gyre, as illustrated schematically in Fig. 4.

Recent advances in understanding have promoted an appreciation for the fully three-dimensional nature of Southern Ocean dynamics (*28*). It is increasingly clear that both physical and biogeochemical processes in the region have a rich zonal structure (*29*, *30*), an understanding of which will be crucial for progressing knowledge of how the Southern Ocean affects global climate on all time scales. The results presented here highlight the crucial role played by cyclonic gyres around the Antarctic continent, the dynamics of which have been broadly absent from historical perspectives on the carbon cycle in the subpolar Southern Ocean.

The conceptual reframing advocated here carries broad implications both for the interpretation of historical research and for the focus of research efforts moving forward. In the first instance, paleoreconstructions of ocean circulation and biogeochemistry are considered almost exclusively through the lens of a two-dimensional framework, consistent with Fig. 1, such that changes in a proxy signal are commonly interpreted to reflect changes in the overturning circulation (*2*, *31*). Our results indicate that processes far removed from the overturning circulation critically affect the biogeochemical signature of deep waters, fundamentally undermining this interpretation. Consideration within the three-dimensional framework of Fig. 4, appreciating the crucial role of the cyclonic gyres, can promote a deeper understanding of the role played by the subpolar Southern Ocean in past changes of the global carbon cycle.

Our results further advocate for a broadening of future research efforts from the biologically productive Antarctic shelf seas, which have been the regions of focus for many process-oriented observational

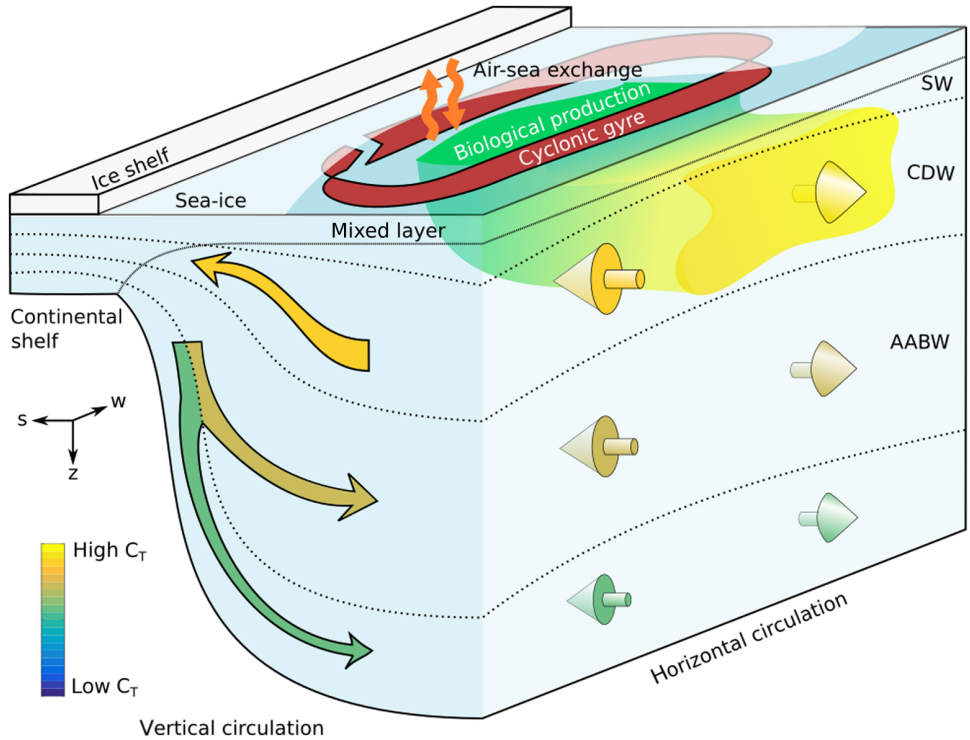

Fig. 4. A three-dimensional perspective of the subpolar Southern Ocean carbon cycle. Schematic illustration of the subpolar Southern Ocean carbon cycle, with the nearside exactly as in Fig. 1 and extended outward to recognize the crucial role of the horizontal circulation of mid-depth waters and their enrichment in carbon by biological production and remineralization in the central gyre region. Dotted lines delineate surface water (SW), CDW, and upper and lower layers of AABW.

campaigns (*15*) and modeling studies (*32*), to the central gyre areas. The physical and biogeochemical controls on the biological carbon pump in these regions are markedly distinct (*18*). As a result, the evolution of each system under future environmental stressors, such as acidification (*33*) and sea-ice cover changes (*34*), may be substantially different.

The primary limitation of this study is that the observational dataset used, while regionally relatively extensive, is specific to a particular window in time. However, broad consistency of the carbon budget with independent measures of carbon uptake suggests that the results are not prohibitively biased by the timing of measurements, on either a seasonal or interannual basis (*17*). With regard to spatial representativeness, it is reasonable to assume that the mechanism of carbon enrichment within the recirculating gyre interior also operates in the other cyclonic gyre systems around the subpolar Southern Ocean (an assumption supported by observations of elevated remineralized carbon in the central Ross Gyre; fig. S4), although the quantitative details will vary between regions. Nonetheless, and as previously highlighted, operation of the mechanism in the Weddell Gyre alone already represents a globally significant drawdown of carbon to the deep ocean. Quantifying contributions from other regions, as well as assessing temporal variations, may be possible in future through analysis of a recent data-assimilating ocean state estimate that includes a carbon cycle (*35*). Further, the impact on the regional carbon cycle of longer time scale variability in both circulation and biogeochemistry, for example, on glacial-interglacial time scales, would be a valuable consideration of future studies.

To conclude, understanding the carbon cycle dynamics of the subpolar Southern Ocean is of critical importance to a number of fundamental, intensely debated questions surrounding the past and future evolution of Earth's climate—from the causes of glacial to interglacial climate transitions (*1*) to future projections of atmospheric CO_2 concentration (*5*). Central to these questions is the permeability of the subpolar Southern Ocean "lid," which mediates exchange with the vast carbon reservoir contained in the lower cell of the global overturning circulation. Our results show that in the present day, it is the coupling of the open-ocean biological pump with the horizontal circulation that is key to maintaining net uptake in the region, thereby keeping the lid closed. We contend, therefore, that efforts to resolve such fundamental questions about Earth's climate are unlikely to succeed as long as the working conceptual framework remains two-dimensional and focused on the overturning circulation. While the sensitivity of the carbon cycle to the overturning circulation is well established (*3*, *4*, *6*), our results show that such a focus crucially misrepresents contemporary observations. The mechanism highlighted in this study indicates a way forward and should be carefully considered within a new three-dimensional framework (Fig. 4).

MATERIALS AND METHODS

Hydrographic and biogeochemical data

Data were collected on three oceanographic transects, plotted in Fig. 2A, that took place over a period of 2 years between 2008 and 2010. Two of the cruises were conducted as part of the Antarctic Deep Water Rates of Export (ANDREX) project in December 2008 to January 2009 and March to April 2010, from the Antarctic Peninsula to 30°E around the northern rim of the Weddell Gyre (*36*, *37*). A third cruise was completed as part of the U.S. CLIVAR (Climate Variability and Predictability) program in February to March 2008 along the quasi-meridional I6S section at 30°E (*38*). Temperature and salinity were measured in 2-dbar pressure bins across the full depth range at each station. Water was collected at an array of depths for onboard measurement of a number of chemical species. Relevant to this study are total dissolved inorganic carbon, total alkalinity, dissolved oxygen, chlorofluorocarbon-11, silicate, and phosphate. For the budget analysis, bottle measurements were optimally interpolated (*39*) onto the hydrographic data points. Full details of the procedure for hydrographic and chemical measurements can be found in the cruise reports, as well as in the studies of Jullion *et al.* (*11*) and Brown *et al.* (*17*).

Inverse model solution

The velocity field used in this analysis was derived by Jullion *et al.* (*11*) via a box inversion. Box inverse modeling facilitates the estimation of large-scale ocean circulation from observations, within a theoretical framework in which conservation of mass, heat, salt, and any other measured tracers can be imposed. Observations of potential temperature, salinity, and pressure, from which potential density is calculated, are used to derive the vertical shear of the cross-section velocity through thermal wind balance. The box inverse method allows the estimation of reference velocities (for each hydrographic station pair) that achieve conservation of heat, freshwater, and mass (equivalently temperature, salinity, and volume, assuming incompressibility) across the full depth and within each of the model layers, with the minimal perturbation (in a least-squares sense) to an a priori estimate. Jullion *et al.* (*11*) used 10 vertical layers based on neutral density (*40*), chosen to delineate the major water masses in the Weddell Gyre. In this inversion, an additional constraint was placed on the net volume and salinity transport of the ACC (0 ± 5 Sv for each), which crosses the corner of the box between stations 82 and 111, to improve the solution. The solution also accounts for the transport of volume, temperature, and freshwater by eddying motions. These terms were derived from time averaging of the Southern Ocean State Estimate (*41*) at the location of the hydrographic sections. In this study, we applied a small correction to the solution of Jullion *et al.* (*11*) to impose full-depth conservation of mass as opposed to volume (the previous solution assumed incompressibility). In applying this correction, we constrained the full-depth carbon transport so that it remained consistent with that of Brown *et al.* (*17*). The correction invoked minimal change in the velocity field, but mass conservation is important for the decomposition of the contributions to carbon transport from the overturning and horizontal circulations.

Uncertainties in carbon transports were determined using Monte Carlo simulations of the inversion-derived velocity field and carbon concentration section. Reference velocities for the inversion were perturbed on the basis of 5-day variability of the velocity field in the Southern Ocean State Estimate (*41*). Carbon concentrations were perturbed within measurement uncertainty (±2 to 3 μmol kg^{-1}) (*17*). The comparatively small uncertainty in the full-depth integral (relative to that of individual layers; see Fig. 3A, taking note of the different *x*-axis ranges) arises from the integral constraints (full-depth mass and salt conservation) applied in the inverse model, which establish statistical dependence of the layer-wise uncertainties. For example, when the sensitivity of the solution is tested to increased inflow (within local uncertainty) in a shallow layer, there must (by conservation of mass and/or salinity) be a corresponding increase of outflow in a deeper layer. Further details can be found in the study of Jullion *et al.* (*11*) and references therein.

Despite being derived from "snapshot" observations, the velocity field is representative of a multi-annual mean state. This follows from the fact that the inverse model was designed to have uncertainties that represent deviations from a long-term mean, as discussed extensively by Jullion *et al.* (*11*). Because of the seasonality of upper ocean

biogeochemistry, carbon transports in the surface water and winter water layers are representative of a summertime mean state, described in detail by Brown *et al.* (*17*). Biogeochemical properties in intermediate and deep layers are stable over the seasonal cycle such that their transports represent a long-term, annual-mean signal. The representativeness of our carbon measurements (and resultant carbon transports) was assessed by Brown *et al.* (*17*) by substituting the modern observations in the inverse model with an alternative, temporally separated section of measurements, thereby directly testing the effect of interannual variability in the carbon field. The carbon transports were found to be robust to such changes, implying that for temporally separated data of the same season, it is the circulation scheme that ultimately sets the state of the carbon residual.

Carbon partitioning formulation

Carbon concentration in a water parcel can be separated into constituent parts using coincidentally measured hydrographic and chemical data (*24*). We provide a summary of the partitioning here and refer to MacGilchrist *et al.* (*25*) for full details. The primary separation is between preformed carbon—the concentration present in the water parcel on leaving the surface—and regenerated carbon—carbon added to the water parcel since leaving the surface ocean. The carbon partitioning is written as

$$C_T = \underbrace{C_{sat}^{pi} + \overbrace{C_{sat}^{ant} + \Delta C}^{C_{res}}}_{\text{preformed}} + \underbrace{C_{soft} + C_{carb}}_{\text{regenerated}} \quad (3)$$

The saturated component ($C_{sat}^{pi} + C_{sat}^{ant}$) is a measure of the carbon concentration that would have been present in the water at the surface were it at equilibrium with the overlying atmosphere. It is separated into "preindustrial" and "anthropogenic" components to account for the changing levels of atmospheric CO_2 since the industrial revolution. The preindustrial saturated component, C_{sat}^{pi}, is determined from potential temperature, salinity, and preformed alkalinity (see below) and was evaluated using the CO2SYS MATLAB program (*42*), assuming a preindustrial atmospheric CO_2 level of 278 ppm. We did not attempt to evaluate the anthropogenic saturated component directly but instead included it in a residual C_{res} along with the disequilibrium component, ΔC, which accounts for the extent to which the water parcel was out of equilibrium with the overlying atmosphere when it left the surface ocean. The regenerated component comprises contributions from the remineralization of soft tissue organic matter, C_{soft}, and the dissolution of hard shell carbonates, C_{carb}. The soft tissue component is established from the apparent oxygen utilization (AOU), itself derived from an estimate of the preformed oxygen concentration: $AOU = O_2 - O_{2,pre}$. We used a carbon-to-oxygen ratio of 117:−170 (*43*). The dissolved carbonate contribution is established from the difference between the measured alkalinity and its preformed value—a function of the surface (upper 100 dbar) salinity-alkalinity relationship (fig. S5). The primary uncertainties in the carbon partitioning formulation relate to the estimation of regenerated carbon and nutrients, both in the necessity to assume a level of oxygen saturation and in the prescription of fixed stoichiometric ratios. In addition, the salinity-alkalinity relationship in the surface ocean can vary widely (*44*). We adopted the simplest approximations possible (100% oxygen saturation, standard stoichiometric ratios, and the local salinity-alkalinity relationship), accepting that there could be quantitative differences in the results if other values were used.

Satellite-derived net primary production

Monthly estimates of net primary production were retrieved at 1/6° × 1/6° latitude-longitude resolution across the area enclosed by the ANDREX-I6S Weddell Gyre sections between 2003 and 2014 from the Ocean Productivity website (http://science.oregonstate.edu/ocean.productivity/index.php). Net primary production was calculated from chlorophyll-a, sea surface temperature (both derived from the Aqua-MODIS satellite data), and photosynthetically active radiation (derived from the SeaWiFS satellite data). Calculations were done using three independent models: the standard and Eppley applications of the Vertical General Productivity Model (*45*) and the Carbon-based Production Model (*46*). The value presented in the main text is the time-mean net primary production for the full time series, with the range representing the spread from the different model calculations.

SUPPLEMENTARY MATERIALS

Supplementary material for this article is available at http://advances.sciencemag.org/cgi/content/full/5/8/eaav6410/DC1

Fig. S1. Transports of the layer-wise carbon anomaly in CDW.
Fig. S2. Carbon partitioning in the Weddell Gyre.
Fig. S3. CFC-11 in the Weddell Gyre.
Fig. S4. Carbon and carbon partitioning in the Ross Sea.
Fig. S5. Salinity-alkalinity relationship in the Weddell Gyre surface ocean.

REFERENCES AND NOTES

1. D. M. Sigman, M. P. Hain, G. H. Haug, The polar ocean and glacial cycles in atmospheric CO_2 concentration. *Nature* **466**, 47–55 (2010).
2. J. Gottschalk, L. C. Skinner, J. Lippold, H. Vogel, N. Frank, S. L. Jaccard, C. Waelbroeck, Biological and physical controls in the Southern Ocean on past millennial-scale atmospheric CO_2 changes. *Nat. Commun.* **7**, 11539 (2016).
3. J. L. Sarmiento, J. R. Toggweiler, A new model for the role of the oceans in determining atmospheric pCO_2. *Nature* **308**, 621–624 (1984).
4. B. B. Stephens, R. F. Keeling, The influence of Antarctic sea ice on glacial-interglacial CO_2 variations. *Nature* **404**, 171–174 (2000).
5. R. Bernardello, I. Marinov, J. B. Palter, E. D. Galbraith, J. L. Sarmiento, Impact of Weddell Sea deep convection on natural and anthropogenic carbon in a climate model. *Geophys. Res. Lett.* , 7262–7269 (2014).
6. R. Ferrari, M. F. Jansen, J. F. Adkins, A. Burke, A. L. Stewart, A. F. Thompson, Antarctic sea ice control on ocean circulation in present and glacial climates. *Proc. Natl. Acad. Sci. U.S.A.* **111**, 8753–8758 (2014).
7. S. Khatiwala, F. W. Primeau, T. M. Hall, Reconstruction of the history of anthropogenic CO_2 concentrations in the ocean. *Nature* **462**, 346–350 (2009).
8. S. M. A. C. van Heuven, M. Hoppema, E. M. Jones, H. J. W. de Baar, Rapid invasion of anthropogenic CO_2 into the deep circulation of the Weddell Gyre. *Philos. Trans. A Math. Phys. Eng. Sci.* **372**, 20130056 (2014).
9. S. Honjo, S. J. Manganini, R. A. Krishfield, R. Francois, Particulate organic carbon fluxes to the ocean interior and factors controlling the biological pump: A synthesis of global sediment trap programs since 1983. *Prog. Oceanogr.* **76**, 217–285 (2008).
10. M. Hoppema, E. Fahrbach, M. H. C. Stoll, H. J. W. de Baar, Annual uptake of atmospheric CO_2 by the Weddell sea derived from a surface layer balance, including estimations of entrainment and new production. *J. Mar. Syst.* **19**, 219–233 (1999).
11. L. Jullion, A. C. N. Garabato, S. Bacon, M. P. Meredith, P. J. Brown, S. Torres-Valdés, K. G. Speer, P. R. Holland, J. Dong, D. Bakker, M. Hoppema, B. Loose, H. J. Venables, W. J. Jenkins, M. J. Messias, E. Fahrbach, The contribution of the Weddell Gyre to the lower limb of the Global Overturning Circulation. *J. Geophys. Res. Oceans* **119**, 3357–3377 (2014).
12. A. H. Orsi, G. C. Johnson, J. L. Bullister, Circulation, mixing and production of Antarctic Bottom Water. *Prog. Oceanogr.* **43**, 55–109 (1999).
13. A. J. Watson, G. K. Vallis, M. Nikurashin, Southern Ocean buoyancy forcing of ocean ventilation and glacial atmospheric CO_2. *Nat. Geosci.* **8**, 861–864 (2015).
14. N. P. Roden, E. H. Shadwick, B. Tilbrook, T. W. Trull, Annual cycle of carbonate chemistry and decadal change in coastal Prydz Bay, East Antarctica. *Mar. Chem.* **155**, 135–147 (2013).
15. E. H. Shadwick, B. Tilbrook, G. D. Williams, Carbonate chemistry in the Mertz Polynya (East Antarctica): Biological and physical modification of dense water outflows and the export of anthropogenic CO_2. *J. Geophys. Res. Oceans* **119**, 1–14 (2014).

16. O. J. Legge, D. C. E. Bakker, M. T. Johnson, M. P. Meredith, H. J. Venables, P. J. Brown, G. A. Lee, The seasonal cycle of ocean-atmosphere CO_2 flux in Ryder Bay, west Antarctic Peninsula. *Geophys. Res. Lett.* **42**, 2934–2942 (2015).
17. P. J. Brown, L. Jullion, P. Landschützer, D. C. E. Bakker, A. C. Naveira Garabato, M. P. Meredith, S. Torres-Valdés, A. J. Watson, M. Hoppema, B. Loose, E. M. Jones, M. Telszewski, S. D. Jones, R. Wanninkhof, Carbon dynamics of the Weddell Gyre, Southern Ocean. *Global Biogeochem. Cycles* **29**, 1–19 (2015).
18. M. Hoppema, R. Middag, H. J. W. de Baar, E. Fahrbach, E. M. van Weerlee, H. Thomas, Whole season net community production in the Weddell Sea. *Polar Biol.* **31**, 101–111 (2007).
19. D. C. E. Bakker, M. Hoppema, M. Schröder, W. Geibert, H. J. W. de Baar, A rapid transition from ice covered CO_2-rich waters to a biologically mediated CO_2 sink in the eastern Weddell Gyre. *Biogeosciences* **5**, 1373–1386 (2008).
20. M. Hoppema, Weddell Sea is a globally significant contributor to deep-sea sequestration of natural carbon dioxide. *Deep. Res. Part I Oceanogr. Res. Pap.* **51**, 1169–1177 (2004).
21. M. Hoppema, Weddell Sea turned from source to sink for atmospheric CO_2 between pre-industrial time and present. *Glob. Planet. Change* **40**, 219–231 (2004).
22. H. L. Bryden, S. Imawaki, in *Ocean Circulation and Climate*, G. Siedler, J. A. Church, J. Gould, Eds. (Academic Press, 2001).
23. A. C. Naveira Garabato, E. L. McDonagh, D. P. Stevens, K. J. Heywood, R. J. Sanders, On the export of Antarctic Bottom Water from the Weddell Sea. *Deep. Res. Part II Top. Stud. Oceanogr.* **49**, 4715–4742 (2002).
24. R. G. Williams, M. J. Follows, *Ocean Dynamics and the Carbon Cycle: Principles and Mechanisms* (Cambridge Univ. Press, 2011).
25. G. A. MacGilchrist, A. C. N. Garabato, T. Tsubouchi, S. Bacon, S. Torres-Valdés, K. Azetsu-Scott, The Arctic Ocean carbon sink. *Deep Sea Res. Part I Oceanogr. Res. Pap.* **86**, 39–55 (2014).
26. M. Hoppema, H. J. W. de Baar, E. Fahrbach, R. G. J. Bellerby, Renewal time and transport of unventilated Central Intermediate Water of the Weddell Sea derived from biogeochemical properties. *J. Mar. Res.* **60**, 677–697 (2002).
27. R. Usbeck, M. Rutgers van der Loeff, M. Hoppema, R. Schlitzer, Shallow remineralization in the Weddell Gyre. *Geochem. Geophys. Geosyst.* **3**, 1–18 (2002).
28. S. R. Rintoul, The global influence of localized dynamics in the Southern Ocean. *Nature* **558**, 209–218 (2018).
29. V. Tamsitt, H. F. Drake, A. K. Morrison, L. D. Talley, C. O. Dufour, A. R. Gray, S. M. Griffies, M. R. Mazloff, J. L. Sarmiento, J. Wang, W. Weijer, Spiraling pathways of global deep waters to the surface of the Southern Ocean. *Nat. Commun.* **8**, 172–181 (2017).
30. N. Gruber, P. Landschützer, N. S. Lovenduski, The variable Southern Ocean carbon sink. *Annu. Rev. Mar. Sci.* **11**, 159–186 (2019).
31. S. L. Jaccard, E. D. Galbraith, A. Martínez-García, R. F. Anderson, Covariation of deep Southern Ocean oxygenation and atmospheric CO_2 through the last ice age. *Nature* **530**, 207–210 (2016).
32. K. R. Arrigo, G. van Dijken, M. Long, Coastal Southern Ocean: A strong anthropogenic CO_2 sink. *Geophys. Res. Lett.* **35**, L21602 (2008).
33. A. J. Fassbender, C. L. Sabine, H. I. Palevsky, Nonuniform ocean acidification and attenuation of the ocean carbon sink. *Geophys. Res. Lett.* **44**, 8404–8413 (2017).
34. M. M. Holland, L. Landrum, Y. Kostov, J. C. Marshall, Sensitivity of Antarctic sea ice to the Southern Annular Mode in coupled climate models. *Climate Dynam.* **49**, 1813–1831 (2017).
35. A. Verdy, M. R. Mazloff, A data assimilatingmodel for estimating Southern Ocean biogeochemistry. *J. Geophys. Res. Ocean.* **122**, 6968–6988 (2017).
36. S. Bacon, L. Jullion, "RRS James Cook: Antarctic deep water rates of export (ANDREX)" (Technical Report 08, National Oceanography Centre, 2009).
37. M. P. Meredith, "Cruise report: RRS James Clark Ross JR235/236/239" (Technical Report, British Antarctic Survey, 2010).
38. K. G. Speer, T. Dittmar, "Cruise report, RV Revelle, 33RR20080204" (Technical Report, Florida State University, 2008).
39. D. Roemmich, Optimal estimation of hydrographic station data and derived fields. *J. Phys. Oceanogr.* **13**, 1544–1549 (1983).
40. D. R. Jackett, T. J. McDougall, A neutral density variable for the world's oceans. *J. Phys. Oceanogr.* **27**, 237–263 (1997).
41. M. R. Mazloff, P. Heimbach, C. Wunsch, An eddy-permitting Southern Ocean state estimate. *J. Phys. Oceanogr.* **40**, 880–899 (2010).
42. S. M. A. C. van Heuven, D. Pierrot, E. Lewis, D. W. R. Wallace, *MATLAB Program Developed for CO2 System Calculations* (ORNL/CDIAC-105b, Carbon Dioxide Information Analysis Center, Oak Ridge National Laboratory, 2009).
43. L. A. Anderson, J. L. Sarmiento, Redfield ratios of remineralization determined by nutrient data analysis. *Global Biogeochem. Cycles* **8**, 65–80 (1994).
44. C. H. Fry, T. Tyrrell, M. P. Hain, N. R. Bates, E. P. Achterberg, Analysis of global surface ocean alkalinity to determine controlling processes. *Mar. Chem.* **174**, 46–57 (2015).
45. M. J. Behrenfeld, P. Falkowski, Photosynthetic rates derived from satellite based chlorophyll concentration. *Limnol. Oceanogr.* **42**, 1–20 (1997).
46. T. Westberry, M. J. Behrenfeld, D. A. Siegel, E. Boss, Carbon-based primary productivity modeling with vertically resolved photoacclimation. *Global Biogeochem. Cycles* **22**, GB2024 (2008).
47. S. Sathyendranath, S. Groom, M. Grant, R. J. W. Brewin, A. Thompson, A. Chuprin, A. Horseman, T. Jackson, V. Martinez Vicente, T. Platt, C. Brockmann, M. Zühlke, R. Doerffer, A. Valente, V. Brotas, H. Krasemann, D. Müller, M. Dowell, F. Mélin, J. Swinton, A. Farman, S. Lavender, T. S. Moore, P. Regner, S. Roy, F. Steinmetz, C. Mazeran, V. E. Brando, M. Taberner, D. Antoine, R. Arnone, W. M. Balch, K. Barker, R. Barlow, S. Bélanger, J.-F. Berthon, Ş. Beşiktepe, E. Canuti, F. Chavez, H. Claustre, R. Crout, R. Frouin, C. García-Soto, S. W. Gibb, R. Gould, S. Hooker, M. Kahru, H. Klein, S. Kratzer, H. Loisel, D. McKee, B .G. Mitchell, T. Moisan, G. Feldman, B. Franz, F. Muller-Karger, L. O'Dowd, M. Ondrusek, A. J. Poulton, M. Repecaud, T. Smyth, H. M. Sosik, M. Twardowski, K. Voss, J. Werdell, M. Wernand, G. Zibordi, *ESA Ocean Colour Climate Change Initiative (Ocean Colour CCI): Global Chlorophyll-a Data Products Gridded on a Geographic Projection, Version 2.0* (Centre for Environmental Data Analysis, 2016).

Acknowledgments: We are grateful to all scientists and support staff involved in the collection and analysis of samples, both at sea and on shore, especially K. Speer, chief scientist of the I06S line occupied as part of the U.S. CLIVAR repeat hydrography program, and H. Venables and P. Abrahamsen for their work on the ANDREX cruises. We are grateful to two anonymous reviewers, whose contributions improved the quality of this manuscript. **Funding:** The ANDREX project was supported by the National Environmental Research Council (NE/E01366X/1 and NE/E013538/1). G.A.M. acknowledges support from NERC, the U.K. Met Office, and a Radcliffe-Graduate scholarship from University College, Oxford. A.C.N.G. acknowledges the support of a Philip Leverhulme Prize, the Royal Society, and the Wolfson Foundation. M.P.M. acknowledges support from NERC via awards NE/N018095/1 and NE/E013368/1. P.J.B. acknowledges support from NERC via award NE/N018095/1. **Author contributions:** G.A.M. performed the analysis (except those aspects noted below), produced the figures, and wrote the manuscript. A.C.N.G. conceived the experimental approach and contributed to the writing of the manuscript. P.J.B. assisted with carbon budget calculations and performed the satellite-based primary production calculations. L.J. evaluated the original inversion-derived velocity field. S.B., D.C.E.B., M.H., M.P.M., and S.T.-V. were all involved in the original data collection. All authors contributed to revising draft manuscripts. **Competing interests:** The authors declare that they have no competing interests, financial or otherwise. **Data and materials availability:** Data for the Weddell Gyre sections are available from the CLIVAR and Carbon Hydrographic Data Office (https://cchdo.ucsd.edu). SOSE data are available from http://sose.ucsd.edu. Ocean color data (used in Fig. 1) are available from www.esa-oceancolour-cci.org. MATLAB scripts for reproducing the analysis are available at http://github.com/gmacgilchrist or by request to the author.

Submitted 5 October 2018
Accepted 18 July 2019
Published 28 August 2019
10.1126/sciadv.aav6410

Citation: G. A. MacGilchrist, A. C. Naveira Garabato, P. J. Brown, L. Jullion, S. Bacon, D. C. E. Bakker, M. Hoppema, M. P. Meredith, S. Torres-Valdés, Reframing the carbon cycle of the subpolar Southern Ocean. *Sci. Adv.* **5**, eaav6410 (2019).

Science Advances

Reframing the carbon cycle of the subpolar Southern Ocean

Graeme A. MacGilchrist, Alberto C. Naveira Garabato, Peter J. Brown, Loïc Jullion, Sheldon Bacon, Dorothee C. E. Bakker, Mario Hoppema, Michael P. Meredith and Sinhué Torres-Valdés

Sci Adv **5** (8), eaav6410.
DOI: 10.1126/sciadv.aav6410